Thermal crosstalk mitigation in a dual-drive Mach-Zehnder Modulator

Souvaraj De[1,2], Ranjan Das[1], Karanveer Singh[1], Younus Mandalawi[1], Thomas Kleine-Ostmann[2], and Thomas Schneider[1]
[1]THz-Photonics Group, Technische Universität Braunschweig, 38106 Braunschweig, Germany
[2]Department High Frequency and Electromagnetic Fields, Physikalisch-Technische Bundesanstalt (PTB), Bundesallee 100, 38116 Braunschweig, Germany

***Abstract*— Dual-drive, PIN-diode based Mach-Zehnder modulators are pivotal for power-efficient and cost-effective CMOS compatible optical transceivers with small footprints. However, the basic chip materials have substantial thermal conductance resulting in thermal crosstalk, which eventually deteriorates the modulator performance in terms of bandwidth and data transmission capabilities. In this work, we simulate and analyze the influence of thermal crosstalk on such a modulator and the mitigation of the same with a deep air trench design. Additionally, we illustrate the improved modulator performance in terms of small-signal bandwidth and eye diagram at higher data rates.**

I. INTRODUCTION

In recent years, the world has seen a surge in data traffic for datacenter (DC) interconnect applications, the optical backbone, and access networks, which can be successfully handled by low-power, integrated transceivers [1]-[3]. Silicon-based photonic integrated circuits (PICs) provide a suitable platform for such designs considering that it is complementary metal-oxide-semiconductor (CMOS) compatible and capable of large-scale integration. Of late, silicon-based Mach-Zehnder modulators (MZMs) with p-i-n junctions have demonstrated high-speed data modulation and efficient bias control [1], very low power consumption [2] and can be used for high-speed digital-to-analog (DAC) transmission [3] as they are compact, uniform, and above all, provide a quite high electro-optic (EO) bandwidth. However, the chip materials like silicon (Si) and silicon dioxide (SiO_2) show a considerable thermal conductance resulting in thermal crosstalk, especially for densely packed electronic-photonic chips. In the research group *Meteracom*, a thorough investigation of the thermal crosstalk in photonic components is targeted to analyze the metrological parameters for future THz communication systems [4]. A suitable method to alleviate thermal crosstalk is the use of oxide-trench [5] and deep-trench [6] designs. A detailed analysis of the thermal crosstalk and its mitigation with an air-filled deep trench design for a single arm of a PIN diode based MZM is discussed in [6].

In this work, we study and analyze the effect of thermal crosstalk in a dual-arm PIN diode based MZM and mitigate the same with a deep trench. Also, we demonstrate the improvement in the modulator bandwidth and the eye diagram at a higher data rate for the deep-trench assisted design.

II. SIMULATION RESULTS

The deep-trench assisted dual-arm PIN diode based MZM with a length of 350 µm is designed on a standard silicon-on-insulator (SOI) platform with a 2 µm thick SiO_2-based buried oxide (BOX) layer. Two 5 µm wide and 0.09 µm thick n^{++} doped Si heaters with doping concentrations of 1×10^{20} cm^{-3} are placed at a separation of $s = 2.5$ µm from the waveguides, which have dimensions of 220 nm × 500 nm. Here, we emulate the worst-case scenario so that the waveguide, as well as the MZM, are heated from both sides. This is a viable scenario in densely packed photonic circuits with a very large number of components. The deep trench [6] separates the modulator from the waveguides at either end. The complete design is implemented using the CHARGE and HEAT solvers of Lumerical [7]. The intrinsic (i) region of the PIN diode is composed of the silicon waveguide core, and it is surrounded on either side by p^+ and n^+ regions with a doping concentration of 2×10^{18} cm^{-3}. The intrinsic regions are separated by a p^+ region with a width of 100 µm. The n^{++} and p^{++} wells have a doping concentration of 5×10^{20} cm^{-3}. The top view and cross-sectional view of the deep-trench assisted device design are depicted in Fig. 1 (a) and (b), respectively. To illustrate the

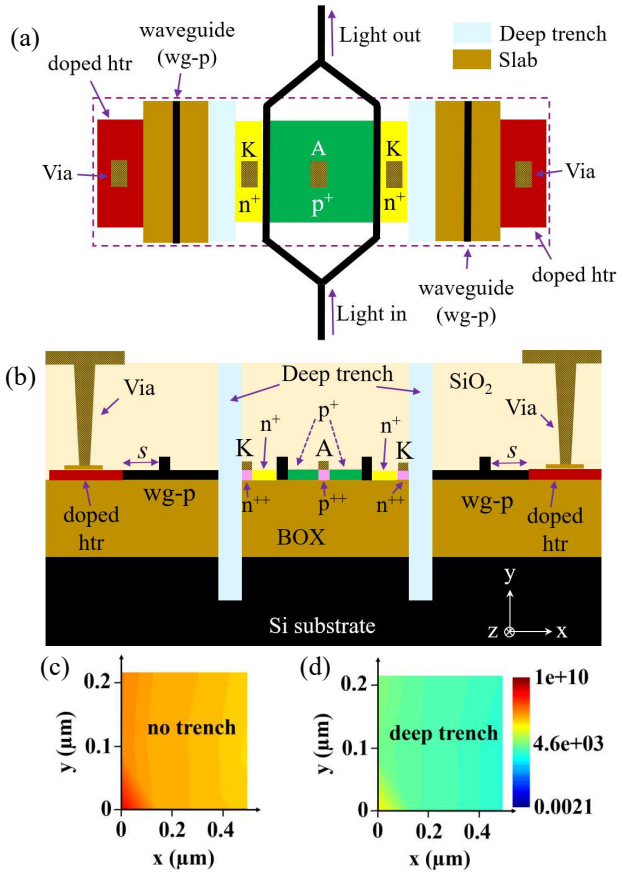

Fig. 1. Schematic (top view (a) and cross-section (b)) of the dual-arm PIN-diode based MZM and waveguide (wg-p) with a deep trench. Please note that the views are not true to scale. Charge profile in the intrinsic (i) region without (c) and with a deep trench (d) at $V_{bias} = 2$ V for a heater power of 260 mW. The color bar shows the n-type charge concentration per cm^3.

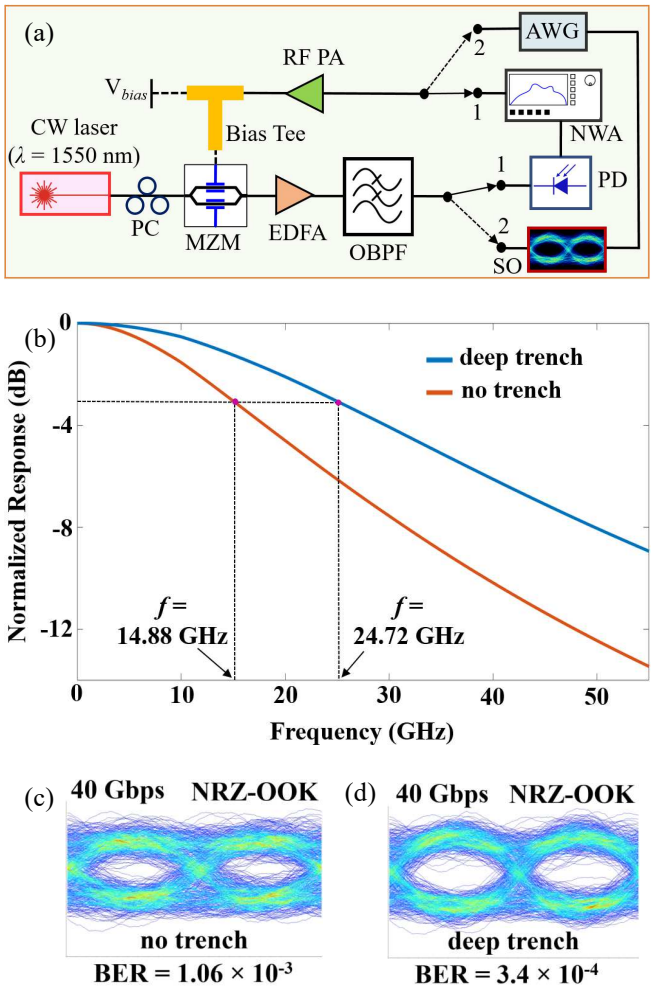

Fig. 2. (a) Schematic diagram of the simulation setup for comparing the bandwidth (switches at position 1) and eye diagram (switches at position 2) consisting of a continuous-wave (CW) laser, polarization controller (PC), dual-arm PIN diode based MZM, erbium-doped fiber amplifier (EDFA), optical bandpass filter (OBPF), photodetector (PD), sampling oscilloscope (SO), network analyzer (NWA), arbitrary waveform generator (AWG), radio frequency Power Amplifier (RF PA), bias tee network, etc. (b) Bandwidth comparison of the dual-arm PIN diode based MZM with 350 µm length for no trench and deep trench design. Eye diagrams of the dual-arm PIN diode based MZM at 40 Gbps for: (c) no trench, and (d) deep trench scenario.

effect of thermal crosstalk, a forward bias voltage V_{bias} of 2 V is applied across the electrodes of the MZM for a heater power of 260 mW. The rising temperature of the heater leads to a temperature increase inside the pin junction, resulting in an increase of the junction capacitance due to the diffusion of n^+ and p^+ charge carriers. However, the deep trench design thermally isolates the MZM and the intrinsic (i) region remains at the ambient temperature of 300 K. As such, the charge concentration in the intrinsic (i) region is much lower compared to the no-trench scenario as seen in Fig. 1 (c) and (d).

To evaluate the device EO bandwidth and eye diagram of the device, simulations are done using the INTERCONNECT solver of Lumerical [7] as per the schematic diagram in Fig. 2 (a). As observed from Fig. 2 (b), the thermal isolation results in higher bandwidth, i.e., 24.72 GHz for the deep trench compared to 14.88 GHz without the trench. Hence, without any external data processing techniques, the device bandwidth improves by 66 %. This is a result of the lower capacitance and resistance due to the reduced charge concentration in the MZM core. Consequently, the time constant is reduced, and the bandwidth is vastly improved. The modulator performance is examined for a data rate of 40 Gbps for a non-return-to-zero on-off keying (NRZ-OOK) modulation scheme as shown in the schematic diagram of Fig. 2 (a). It is seen that without a trench, the dual-arm PIN diode based MZM has a higher bit error rate (BER) of 1.06×10^{-3} with a narrow eye opening. But, for the deep trench, the BER is 3.4×10^{-4} with a much wider eye opening. Therefore, the proposed deep-trench assisted dual-arm PIN diode based MZM design has a better performance than the regular design.

III. SUMMARY

This work demonstrates that a deep trench can alleviate thermal crosstalk in densely packed photonic circuits involving dual-arm PIN-diode based MZMs. Moreover, with a deep trench, the device bandwidth is increased by 66 %, and the BER is improved without using any further complex procedures. The next phase of our work involves an experimental validation of the proposed design.

ACKNOWLEDGEMENT

This work is funded by the Deutsche Forschungsgemeinschaft (DFG, German Research Foundation) (403579441, 424608109, 424608271, 424607946, 424608191, 403154102, 322402243).

REFERENCES

[1] G. -W. Lu, *et al.*, "Power-Efficient O-Band 40 Gbit/s PAM4 Transmitter Based on Dual-Drive Cascaded Carrier-Depletion and Carrier-Injection Silicon Mach-Zehnder Modulator With Binary Driving Electronics at CMOS Voltages," in *IEEE Journal of Selected Topics in Quantum Electronics*, vol. **27**, no. 3, pp. 1-8, 2021.

[2] S. Tanaka, *et al.*, "Ultralow-Power (1.59 mW/Gbps), 56-Gbps PAM4 Operation of Si Photonic Transmitter Integrating Segmented PIN Mach–Zehnder Modulator and 28-nm CMOS Driver," in *Journal of Lightwave Technology*, **36**, no. 5, pp. 1275-1280, 2018.

[3] Y. Sobu, *et al.*, "High-Speed Optical Digital-to-Analog Converter Operation of Compact Two-Segment All-Silicon Mach–Zehnder Modulator," in *Journal of Lightwave Technology*, **39**, no. 4, pp. 1148-1154, 2021.

[4] D. Humphreys *et. al.*, "An overview of the Meteracom Project", *Proc. 43rd Wireless World Research Forum (WWRF 2019)*, London, UK, Oct. 2019.

[5] S. De, R. Das, R. K. Varshney and T. Schneider, "Design and Simulation of Thermo-Optic Phase Shifters With Low Thermal Crosstalk for Dense Photonic Integration," in *IEEE Access*, vol. **8**, pp. 141632-141640, 2020.

[6] S. De, R. Das, R. K. Varshney and T. Schneider, "CMOS-Compatible Photonic Phase Shifters With Extremely Low Thermal Crosstalk Performance," in *Journal of Lightwave Technology*, **39**, 2113-2122, (2021).

[7] Lumerical Inc. https://www.lumerical.com/products.